MEIS1-regulated miR-488-3p suppresses the malignant progression of laryngeal squamous cell carcinoma by targeting ACVR1C

CHUNMING ZHANG[1-3*], WENJING HAO[1,4*], XINFANG WANG[1,4*], HUINA GUO[1,2], LONG HE[1,2], JIAO YANG[5], YING WANG[1,2], XIWANG ZHENG[1,2], ZHONGXUN LI[1,2], QI HAN[1,2], LIQI WEN[1,2] and HONGLIANG LIU[1-4]

[1]Shanxi Key Laboratory of Otorhinolaryngology Head and Neck Cancer, First Hospital of Shanxi Medical University, Taiyuan, Shanxi 030001, P.R. China; [2]Shanxi Province Clinical Medical Research Center for Precision Medicine of Head and Neck Cancer, First Hospital of Shanxi Medical University, Taiyuan, Shanxi 030001, P.R. China; [3]Department of Otolaryngology Head and Neck Surgery, First Hospital of Shanxi Medical University, Taiyuan, Shanxi 030001, P.R. China; [4]Department of Cell Biology and Genetics, The Basic Medical School of Shanxi Medical University, Taiyuan, Shanxi 030001, P.R. China; [5]Department of Anatomy, The Basic Medical School of Shanxi Medical University, Taiyuan, Shanxi 030001, P.R. China

Received March 28, 2025; Accepted July 4, 2025

DOI: 10.3892/ijmm.2025.5583

Abstract. Laryngeal squamous cell carcinoma (LSCC) is a common malignant tumor originating from the mucosal epithelium of the larynx. MicroRNA (miR)-488-3p has non-negligible multifaceted roles in some types of cancer; however, its association with LSCC has not yet been reported. Our prior RNA sequencing data indicated that miR-488-3p expression is downregulated in LSCC tissue, yet the detailed function and regulatory mechanism of miR-488-3p in LSCC remain unknown. In the present study, quantitative PCR analysis corroborated the significant downregulation of miR-488-3p in LSCC tumor tissues, with this downregulation being strongly associated with malignant progression in LSCC. Furthermore, overexpression of miR-488-3p suppressed LSCC cell proliferation, colony formation, migration, invasion, xenograft tumor growth and epithelial-mesenchymal transition. Mechanistically, miR-488-3p directly interacted with the 3' untranslated region of activin A receptor type 1C (ACVR1C) and downregulated ACVR1C expression. Functional experiments revealed that miR-488-3p suppressed the malignant phenotypes of LSCC via ACVR1C. Additionally, bioinformatics analysis coupled with chromatin immunoprecipitation assay revealed that myeloid ecotropic viral integration site 1 (MEIS1) promoted the expression of miR-488-3p transcriptionally by directly binding its promoter region. Collectively, the results demonstrated that miR-488-3p acts as a tumor suppressor molecule in LSCC, and a role was established for the MEIS1/miR-488-3p/ACVR1C axis in regulating LSCC progression, thus providing novel potential biomarkers and targets for patients with LSCC.

Correspondence to: Professor Hongliang Liu or Dr Liqi Wen, Shanxi Key Laboratory of Otorhinolaryngology Head and Neck Cancer, First Hospital of Shanxi Medical University, 85 South Jiefang Road, Taiyuan, Shanxi 030001, P. R. China
E-mail: liuhl2018@sxent.org
E-mail: wenliqi@sxent.org

*Contributed equally

Key words: microRNA-488-3p, myeloid ecotropic viral integration site 1, activin A receptor type 1C, laryngeal squamous cell carcinoma

Introduction

Laryngeal squamous cell carcinoma (LSCC) represents a common type of highly aggressive malignant tumor, the incidence and mortality rates of which are increasing annually (1,2). Early stage LSCC (T1 and T2 tumors) is often curable, with a cure rate of 80-90%, whereas the survival rate is ~40% in patients with stage IV LSCC at diagnosis (3). This decline is mainly attributed to the propensity of LSCC for local invasion and metastasis to cervical lymph nodes (4); however, the molecular mechanisms underlying LSCC tumorigenesis, invasion and metastasis are still poorly understood. Therefore, detailed knowledge of the regulatory mechanisms involved in the progression of LSCC is needed for its clinical treatment.

MicroRNAs (miRNAs/miRs) are a class of short non-coding RNA molecules 18-24 nucleotides in length, which primarily bind to the 3' untranslated region (UTR) of mRNA to influence its stability or translation. Dysregulated miRNAs have been reported to affect the development and metastasis of multiple types of cancer, including LSCC (5,6). miR-488-3p, a miRNA generated from the gene located at 1q25.2, has been shown to serve critical roles in multiple aspects of cancer development and progression (7-10). To date, to the best of our knowledge, the biological functions and underlying molecular mechanisms of miR-488-3p in LSCC remain unknown.

Our previous RNA sequencing (RNA-seq) data showed that miR-488-3p expression was markedly decreased in LSCC

tissues compared with that in adjacent normal mucosa (ANM) tissues (11). The present study assessed the expression levels of miR-488-3p in a cohort of LSCC specimens, and investigated the biological functions and regulatory mechanisms of miR-488-3p in LSCC, with the aim of providing insight into the effects of miR-488-3p on LSCC progression and highlighting its significance in LSCC diagnosis and treatment.

Materials and methods

Tissue samples and ethics statement. A total of 65 paired LSCC and matched ANM tissue samples were collected between January 2021 and July 2024 from surgical patients at the Department of Otolaryngology Head and Neck Surgery, First Hospital of Shanxi Medical University (Taiyuan, China). All tissue samples were collected after obtaining written informed consent from patients. Fresh specimens were immediately frozen using liquid nitrogen for quantitative PCR (qPCR) analysis. The present study was approved by the Ethics Committee of the First Hospital of Shanxi Medical University (approval no. 2021-K-K005). The detailed clinical characteristics of the patients with LSCC are listed in Table SI.

Cell culture. The AMC-HN-8 cell line was obtained from The Cell Bank of Type Culture Collection of The Chinese Academy of Sciences. The FD-LSC-1 cells were provided by Professor Liang Zhou (Eye, Ear, Nose and Throat Hospital, Fudan University, Shanghai, China) (12). 293T cells and the embryonic lung fibroblast diploid cell line 2BS were purchased from China Center for Type Culture Collection. 293T and AMC-HN-8 cells were cultured in DMEM (Gibco; Thermo Fisher Scientific, Inc.) supplemented with 10% fetal bovine serum (FBS; Biological Industries; Sartorius AG). FD-LSC-1 and 2BS cells were cultured in Bronchial Epithelial Cell Growth Medium (Lonza Group, Ltd.) and MEM (Procell Life Science &Technology Co., Ltd.) with 10% FBS, respectively. All cells were cultured at 37˚C with 5% CO_2.

miRNA mimics, inhibitor, agomir and small interfering RNA (siRNA). miR-488-3p mimics (forward, 5'-UUG AAAGGCUAUUUCUUGGUC-3' and reverse, 5'-GAC CAAGAAAUAGCCUUUCAA-3'), miR-488-3p inhibitor (5'-GACCAAGAAAUAGCCUUUCAA-3'), miR-488-3p agomir (forward, 5'-UUGAAAGGCUAUUUCUUGGUC-3' and reverse, 5'-GACCAAGAAAUAGCCUUUCAA-3'), siRNAs targeting activin A receptor type 1C (ACVR1C) (si-ACVR1C-1; Forward, 5'-GGGCUCCUUAUAUGACUA UTT-3' and reverse, 5'-AUAGUCAUAUAAGGAGCCCTT-3'; si-ACVR1C-2: Forward, 5'-GAGCUGGCCAUCAUUAUU ATT-3' and reverse, 5'-UAAUAAUGAUGGCCAGCUCTT-3'), negative control (NC) mimics (forward, 5'-UUGUACUAC ACAAAAGUACUG-3', and reverse, 5'-CAGUACUUUUGU GUAGUACAA-3'), NC inhibitor (5'-CAGUACUUUUGU GUAGUACAA-3'), NC agomir (forward, 5'-UUGUACUAC ACAAAAGUACUG-3', and reverse, 5'-CAGUACUUUUGU GUAGUACAA-3'), and NC siRNA (forward, 5'-GCGACG AUCUGCCUAAGAUdTdT-3', and reverse, 5'-AUCUUA GGCAGAUCGUCGCdTdT-3') were obtained from Shanghai GenePharma Co., Ltd. For transfection, FD-LSC-1 or AMC-HN-8 cells were seeded in six-well plates at a density of $5x10^5$ cells/well. A total of 5 μl Lipofectamine® 3000 reagent (Invitrogen; Thermo Fisher Scientific, Inc.) and 100 nM miRNA mimics, miRNA inhibitors or siRNAs were mixed in 250 μl Opti-MEM™ (Gibco; Thermo Fisher Scientific, Inc.) and added to each well. Following 4-6 h of incubation at 37˚C with 5% CO_2, the medium was replaced with fresh medium. A total of 48 h post-transfection, the cells were collected for use in subsequent experiments.

Vector construction and cell transfection. Full-length coding sequences of human ACVR1C and myeloid ecotropic viral integration site 1 (MEIS1) were selected and inserted into the p3xFLAG-CMV-10 vector (Sigma-Aldrich; Merck KGaA) for overexpression. The wild-type (WT) and mutant (Mut) ACVR1C 3' UTR sequences were cloned into psiCHECK-2 vector (Promega Corporation) for the dual-luciferase reporter assay. To validate the MEIS1-binding site in the miR-488 promoter, the core region (-2,000 to -1) of the miR-488 promoter was inserted into pGL3-Basic vector (Promega Corporation) to construct the pGL3-488-WT vector. In addition, the core sequence (TGACA) corresponding to the MEIS1-binding site in the miR-488 core promoter was mutated into 'ACTGT' for pGL3-488-Mut vector construction. For plasmid transfection, FD-LSC-1 or AMC-HN-8 cells were seeded in six-well plates at a density of $5x10^5$ cells/well. A total of 5 μl Lipofectamine 3000 reagent and 2.5 μg plasmid vector were mixed in 250 μl Opti-MEM™ and added to each well. Following 4-6 h of incubation at 37˚C with 5% CO_2, the medium was replaced with fresh medium. A total of 48 h following transfection, the cells were collected for use in subsequent experiments.

Reverse transcription (RT)-qPCR. TRIzol® reagent (Invitrogen; Thermo Fisher Scientific, Inc.) was used to isolate total RNA from 2BS cells, 293T cells, and LSCC cell lines (FD-LSC-1 and AMC-HN-8) or tissues. The HiScript II 1st Strand cDNA Synthesis kit (Vazyme Biotech Co., Ltd.) was used to synthesize cDNA from mRNA according to the following conditions: 25˚C for 5 min, 50˚C for 15 min and 85˚C for 2 min. For RT of miRNA, cDNA was synthesized using the All-in-One™ miRNA First-Strand cDNA Synthesis Kit (GeneCopoeia, Inc.) according to the following conditions: 37˚C for 60 min and 85˚C for 5 min. A qPCR Mix (TransGen Biotech Co., Ltd.) and primers (Table SII) were used for the quantitative analysis of mRNA and miRNA. The following thermocycling conditions were used: 95˚C for 30 sec, followed by 40 cycles at 95˚C for 5 sec and 60˚C for 10 sec. Data were normalized to the levels of the internal control and calculated using the $2^{-\Delta\Delta Cq}$ method (13), where 18S rRNA was used as a control for mRNA and U6 snRNA as a control for miRNA.

Cell Counting Kit-8 (CCK-8) and colony formation assays. To observe cell proliferation, $3x10^3$/well FD-LSC-1 cells or $5x10^3$/well AMC-HN-8 cells were seeded in 96-well plates. Subsequently, each well was replaced with 100 μl fresh complete medium and 10 μl CCK-8 reagent (TransGen Biotech Co., Ltd.) at the indicated times (0, 24, 48, 72 and 96 h after seeding) and the cells were incubated at 37˚C for 1-2 h. The absorbance of the solution was then measured at 450 nm

using a Spectra Max i3x Multifunctional microplate detection system (Molecular Devices, LLC). A total of three independent experiments were performed.

For the colony formation assay, 800 LSCC cells/well were seeded into 6-well plates and cultured for 12 days; the medium was changed every 2-3 days. The cell colonies were then fixed with 4% paraformaldehyde at room temperature for 30 min and stained with 0.1% crystal violet (Amresco, LLC) at room temperature for 15 min. Colonies were defined as clusters of >50 cells and the colonies were counted using ImageJ software (version 1.51j8; National Institutes of Health).

Transwell assay. LSCC cells were collected and resuspended in serum-free medium. For the migration assay, $8x10^4$ cells in 200 μl serum-free medium were seeded in the 24-well Transwell (8-μm pore size) upper chamber, and 500 μl medium supplemented with 20% FBS was added to the lower chamber. Likewise, for the invasion assay, $1.2x10^5$ cells in 200 μl serum-free medium were introduced to the upper chamber, which had been precoated with Matrigel (BD Biosciences) at 37˚C for 2 h. After 48 h of incubation at 37˚C with 5% CO_2, the remaining cells in the upper chamber were removed with cotton swabs, and the lower side of the chamber was gently washed twice with PBS and fixed with 4% paraformaldehyde for 30 min at room temperature. The migratory or invasive cells were subsequently stained with 0.1% crystal violet for 15 min at room temperature, and images were captured using a light microscope (Leica Microsystems GmbH).

Prediction of miR-488-3p targets. TargetScan 8.0 (targetscan.org/vert_80/) (14), miRDB (mirdb.org/miRDB/) (15) and miRWalk 2 (mirwalk.umm.uni-heidelberg.de/) (16) were used to predict the downstream target genes of miR-488-3p. The online website Venny (bioinfogp.cnb.csic.es/tools/venny/) was used to identify miR-488-3p target genes common to all three databases (TargetScan, miRDB and miRWalk).

Luciferase reporter assay. To determine the 3' UTR activity of ACVR1C, the WT or Mut ACVR1C 3' UTR reporter vector and miR-488-3p mimics or inhibitor were co-transfected into 293T cells using Lipofectamine 3000 reagent. In addition, the 293T cells were also co-transfected with the pGL3-488-WT/Mut vector and MEIS1 overexpression vector using Lipofectamine 3000 reagent to analyze miR-488 promoter activity. Following co-transfection for 6 h, the culture medium was changed to complete medium, and the transfected cells continued to be cultured at 37˚C in 5% CO_2 for 48 h. Then the cells were lysed and the luciferase activity was detected using a Dual-Luciferase Reporter Assay System (Promega Corporation) according to the manufacturer's instructions. Firefly luciferase activity was normalized to *Renilla* luciferase activity.

Western blotting (WB). The Pierce RIPA lysis buffer (Thermo Fisher Scientific, Inc.) containing protease inhibitor cocktail was used for total protein isolation from LSCC cells. The protein concentration was determined using a BCA Protein Assay kit (Thermo Fisher Scientific, Inc.). An equal concentration of protein was then separated by SDS-PAGE gels and transferred onto PVDF membranes. The membranes were probed with primary antibodies overnight at 4˚C after blocking with 10% w/v skimmed milk for 2-4 h. The next day, after rinsing in Tris-buffered saline containing 0.1% Tween-20, the PVDF membranes were covered with the corresponding secondary antibodies at room temperature for 2 h. The blots were visualized using WesternBright® ECL HRP substrate (Advansta, Inc.). The primary antibodies used were as follows: ACVR1C (1:1,000; cat. no. NBP1-50659; Novus Biologicals, LLC), N-cadherin (1:1,000; cat. no. 13116S; Cell Signaling Technology, Inc.), E-cadherin (1:1,000; cat. no. 3195S; Cell Signaling Technology, Inc.), vimentin (1:1,000; cat. no. 5741S; Cell Signaling Technology, Inc.), Flag (1:1,000; cat. no. F1804; Sigma-Aldrich; Merck KGaA) and GAPDH (1:1,000; cat. no. HC301-02; TransGen Biotech Co., Ltd.). The secondary antibodies used were HRP-conjugated goat anti-rabbit IgG (H+L) (1:1,000; cat. no. A0208; Beyotime Institute of Biotechnology) and HRP-conjugated goat anti-mouse IgG (H+L) (1:1,000; cat. no. A0216; Beyotime Institute of Biotechnology).

Chromatin immunoprecipitation (ChIP) assay. The EZ ChIP™ kit (MilliporeSigma) was used to perform the ChIP assay according to the manufacturer's instructions. Briefly, FD-LSC-1 and AMC-HN-8 cells were subjected to crosslinking using 1% paraformaldehyde at 37˚C for 10 min. The crosslinking process was terminated by the addition of glycine to achieve a final concentration of 0.125 M, incubated for 5 min at room temperature. Subsequently, the crosslinked cells were harvested and lysed in 500 μl SDS lysis buffer supplemented with a protease inhibitor cocktail. Post-lysis, the crosslinked DNA was sonicated to yield fragments 200-500 base pairs in length. Cellular debris was eliminated through centrifugation at 10,000 x g for 10 min at 4˚C. The supernatant lysates were precleared using Protein-A/G agarose beads, followed by immunoprecipitation with 10 μg ChIP-grade antibody against MEIS1 (1:100; cat. no. ab19867; Abcam) or 1 μg IgG control antibody (1:500; cat. no. A7016; Beyotime Institute of Biotechnology) at 4˚C overnight. Subsequently, 60 μl Protein A/G-agarose beads were introduced, and the mixture was subjected to rotation for 2 h at 4˚C. The immunoprecipitated complexes, bound to the beads, were collected via centrifugation at 500 x g for 1 min at 4˚C and underwent sequential washes in a low salt buffer, a high salt buffer, a LiCl buffer, and finally, twice in 1 ml Tris-EDTA buffer. The chromatin bound to beads was eluted using 2x150 μl elution buffer at room temperature. DNA-protein crosslinking was reversed by the addition of NaCl to a final concentration of 0.2 M, followed by incubation at 65˚C overnight. The following day, all samples were treated with RNase at 37˚C for 30 min and proteinase K at 55˚C for 2 h. The liberated DNA was subsequently purified using spin columns provided with the kit. The enrichment of DNA fragments was measured by qPCR, as aforementioned, and electrophoresis on a 2% agarose gel containing 0.5% GelRed Nucleic Acid Gel Stain (Biotium, Inc.). Primer-01 was employed to amplify the miR-488 promoter region, which includes two MEIS1 binding sites. Conversely, Primer-NC served as a NC, amplifying the miR-488 promoter region devoid of the MEIS1 binding site. ChIP primer sequences are presented in Table SII.

Xenograft model generation. The animal experiments were approved by the Ethics Committee for Research Involving Animals of the First Hospital of Shanxi Medical University (approval no. DWYJ-2024-026). A total of 12 female specific pathogen-free-grade nude mice (age, 4-6-weeks; weight, 13-17 g) were obtained from Beijing Vital River Laboratory Animal Technology Co., Ltd. To generate the xenograft models of LSCC, $2x10^6$ FD-LSC-1 cells in 100 μl PBS were injected subcutaneously into the flank of each nude mice. From day 10, xenograft-bearing nude mice were randomized into two groups (n=6 mice/group); one group of mice received 10 nmol miR-488-3p agomir intratumor every 2 days and the other group received an equal volume of NC agomir. Tumor volumes were measured every 2 days until the mice were euthanized by isoflurane inhalation (5%) followed by decapitation on day 22 after inoculation. The humane endpoints were as follows: i) Tumor growth reaching >10% of the body weight or the average tumor diameter in mice surpassing 20 mm; ii) weight loss exceeding 20% of the initial body weight; iii) the mice exhibiting signs of significant pain and distress. No mice reached any of these humane endpoints during the study. The tumor volume was calculated as $V=(a \times b^2)/2$, where a represents the maximum diameter and b the shortest diameter. The excised tumors were weighed, images were captured, and they were embedded in paraffin for immunohistochemical (IHC) staining.

IHC staining. IHC staining was carried out as previously reported (4). Briefly, xenograft tumor tissues were fixed in formaldehyde, embedded paraffin and cut into 5-μm sections. After dewaxing, rehydration, antigen repair and endogenous peroxidase blocking, the sections were immunostained with primary antibodies against E-cadherin (1:200; cat. no. 3195S; Cell Signaling Technology, Inc.), vimentin (1:200; cat. no. 5741S; Cell Signaling Technology, Inc.), N-cadherin (1:100; cat. no. 13116S; Cell Signaling Technology, Inc.) and Ki67 (1:100; cat. no. RMA-0731; Fuzhou Maixin Biotech. Co., Ltd.) at 4˚C overnight. After covering with the corresponding secondary antibody at 37˚C for 15-30 min, the sections were stained with hematoxylin and DAB solution for 10 min at 37˚C. The secondary antibody used was from the Universal kit (mouse/rabbit polymer detection system) (cat. no. PV-6000; OriGene Technologies, Inc.). The neutral gum-sealed sections were then scanned and analyzed using Panoramic Digital Slide Scanner and CaseViewer (version 2.3) (both from 3DHISTECH, Ltd.).

LASAGNA-Search and JASPAR analysis. LASAGNA-Search 2.0 is a web tool that identifies potential transcription factor binding sites in DNA sequences (17). JASPAR2024 (jaspar.elixir.no/) is an open access database of curated, non-redundant transcription factor-binding profiles (18). LASAGNA-Search 2.0 and JASPAR were used to predict the MEIS1-binding sites in the core region of the miR-488 promoter.

Data and sequence acquisition. The mRNA expression data of ACVR1C and MEIS1 in both LSCC and ANM tissues (GSE127165) (11) were extracted from the Gene Expression Omnibus (GEO) database (https://www.ncbi.nlm.nih.gov/geo/). The expression data of miR-488-3p in both LSCC and ANM tissues were extracted from the GEO dataset GSE133632 (11). The promoter sequence (-2,000/-1) of miR-488 was downloaded from the UCSC Genome Browser (https://genome-store.ucsc.edu/) (19).

Statistical analysis. GraphPad Prism (version 8; Dotmatics) was employed to perform the statistical analysis. A two-tailed Student's t-test was used to evaluate the significance between two experimental groups. One-way analysis of variance followed by Tukey's test was used to determine the difference between more than two groups of data. Correlation was analyzed by Pearson's correlation coefficient. Experimental data are presented as the mean ± SD. $P<0.05$ was considered to indicate a statistically significant difference.

Results

Downregulation of miR-488-3p is associated with malignant progression in LSCC. Previous RNA-seq data showed that miR-488-3p expression levels are notably downregulated in LSCC tissue compared with those in ANM tissues (11). In the present study, the expression levels of miR-488-3p were further evaluated in 65 paired LSCC and ANM tissues using RT-qPCR. As shown in Fig. 1A and B, the expression levels of miR-488-3p were significantly lower in LSCC tissues. Furthermore, clinical data displayed that miR-488-3p expression was significantly associated with T stages (20), clinical stages and lymph node metastasis, but not with the degree of differentiation (Fig. 1C-F). A comparison of miR-488-3p expression in FD-LSC-1 and AMC-HN-8 LSCC cells with normal 2BS cells revealed significantly lower miR-488-3p expression in LSCC cells (Fig. 1G). These results highlighted the downregulation of miR-488-3p in LSCC and suggested its critical role in LSCC progression.

miR-488-3p inhibits LSCC cell proliferation, migration, invasion and epithelial-mesenchymal transition (EMT). To explore the potential effects of miR-488-3p on LSCC, the LSCC cells AMC-HN-8 and FD-LSC-1 were transfected with miR-488-3p mimics to induce its overexpression. As shown in Fig. 2A, RT-qPCR indicated that miR-488-3p was overexpressed in the miR-488-3p mimics group compared with that in the NC group. The results of the CCK-8 assay confirmed that miR-488-3p overexpression in AMC-HN-8 and FD-LSC-1 cells reduced their proliferation rates compared with those in the NC group (Fig. 2B). Colony formation assays revealed that the colony formation capacity of LSCC cells was significantly reduced by miR-488-3p overexpression (Fig. 2C). In addition, Transwell assays indicated that upregulation of miR-488-3p significantly inhibited LSCC cell migration and invasion (Fig. 2D and E). To explore the underlying mechanism, the effects of miR-488-3p on the expression levels of EMT markers were investigated. As shown in Fig. 2F, the expression levels of vimentin and N-cadherin were decreased, whereas those of E-cadherin were increased in miR-488-3p-overexpressing LSCC cells compared with in NC-transfected cells, suggesting that upregulation of miR-488-3p may suppress EMT progression in LSCC. Collectively, these findings suggested that miR-488-3p could inhibit LSCC cell proliferation, migration, invasion and EMT.

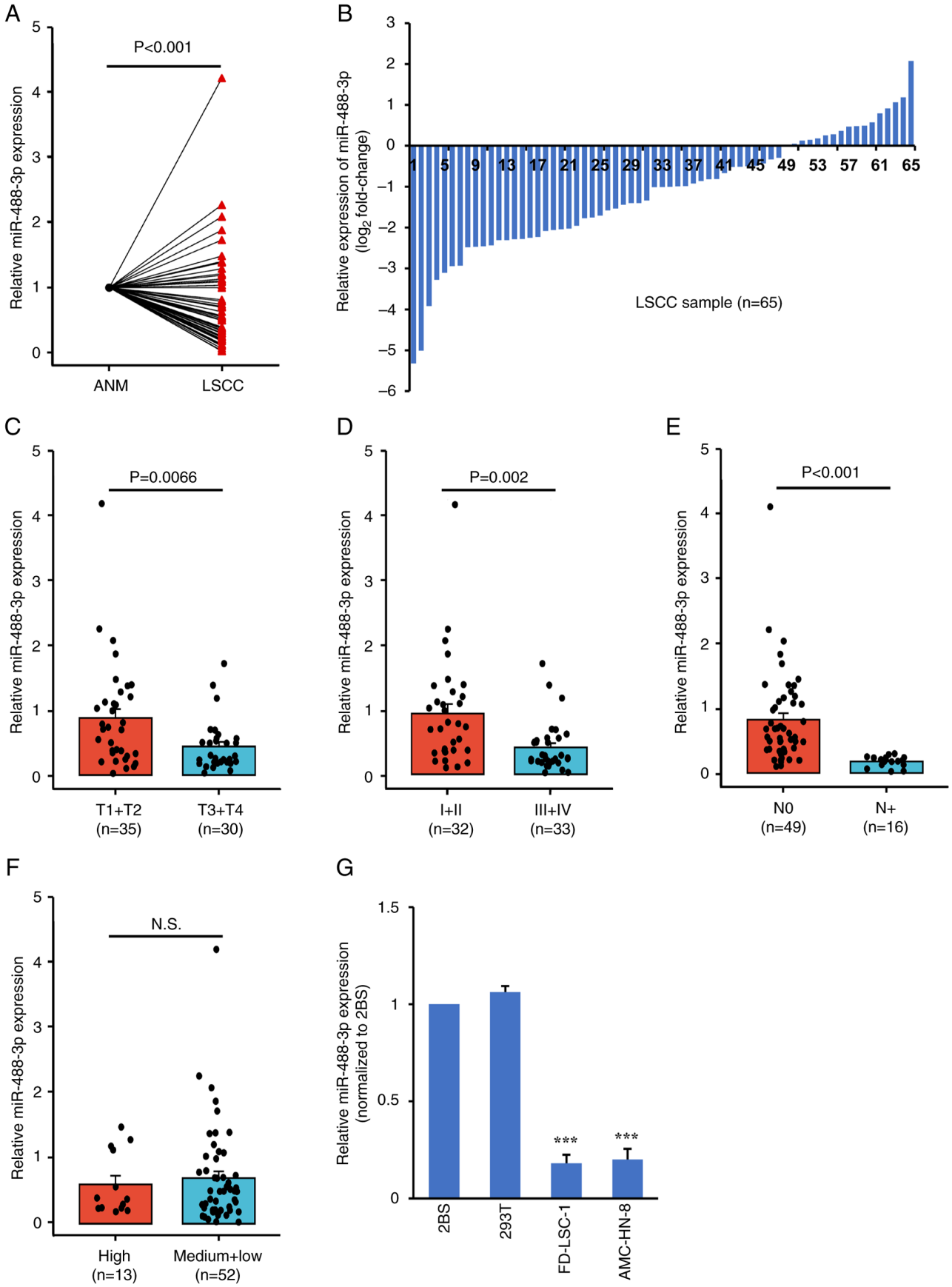

Figure 1. Downregulation of miR-488-3p and its clinical significance in LSCC. The expression levels of miR-488-3p were detected by qPCR in 65 paired LSCC and ANM samples. (A) Comparison of miR-488-3p expression between LSCC and matched ANM samples. (B) Expression levels of miR-488-3p in 65 paired LSCC and matched ANM tissues. Analysis of association between miR-488-3p expression and (C) T stages, (D) clinical stages, (E) lymph node metastasis (N stages) and (F) degree of differentiation. (G) qPCR analysis of miR-488-3p expression in human LSCC and normal cell lines. A comparison of miR-488-3p expression in LSCC FD-LSC-1 and AMC-HN-8 cells with normal revealed significantly lower miR-488-3p expression in LSCC cells. ***P<0.001 vs. 2BS cells. miR, microRNA; LSCC, laryngeal squamous cell carcinoma; qPCR, quantitative PCR; ANM, adjacent normal mucosa; N.S., not significant.

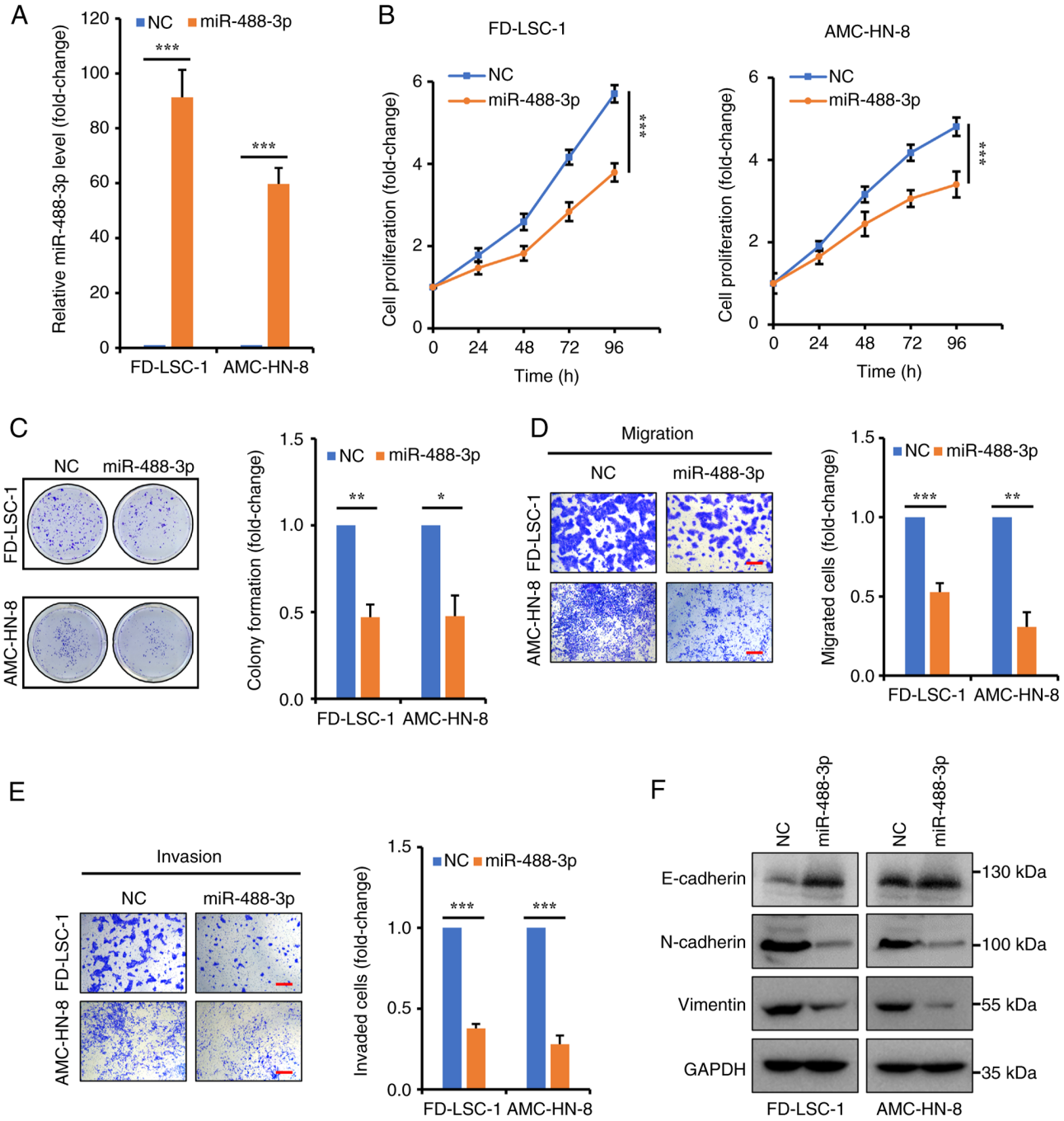

Figure 2. miR-488-3p overexpression inhibits LSCC cell proliferation, migration, invasion and epithelial-mesenchymal transition. (A) Quantitative PCR analysis of miR-488-3p expression in LSCC cells transfected with miR-488-3p or NC mimics. (B) Cell Counting Kit-8 and (C) colony formation assays detected the proliferative ability of LSCC cells transfected with miR-488-3p or NC mimics. Transwell assays determined the (D) migration and (E) invasion of LSCC cells transfected with miR-488-3p or NC mimics. (F) Western blotting of the protein levels of E-cadherin, N-cadherin and vimentin. Cropped images represent different blots, but samples are from the same experiment and the blots were processed in parallel. Scale bars, 100 μm. *P<0.05, **P<0.01 and ***P<0.001. miR, microRNA; LSCC, laryngeal squamous cell carcinoma; NC, negative control.

miR-488-3p directly targets ACVR1C in LSCC. TargetScan, miRDB and miRWalk were used to identify direct target genes for miR-488-3p, resulting in 439, 821 and 5,899 genes, respectively. Venn analysis of the aforementioned three sets of potential target genes obtained 93 common genes (Fig. 3A). Based on previous RNA-seq data, 1,497 genes were obtained that were significantly upregulated in LSCC tissues compared with in ANM tissues (11). Venn analysis of the 93 predicted miR-488-3p target genes and 1,497 upregulated genes obtained four genes, including ACVR1C, ABCA12, TNFSF11 and SYT14 (Fig. 3B). Next, the expression of the aforementioned four genes was detected by RT-qPCR analysis in miR-488-3p-overexpressing cells. The results indicated that only ACVR1C mRNA was significantly reduced in miR-488-3p-overexpressing LSCC cells (Fig. 3C). Furthermore, WB results demonstrated that the protein levels of ACVR1C were also markedly reduced in miR-488-3p-overexpressing LSCC cells (Fig. 3D). To verify that miR-488-3p directly binds to ACVR1C 3' UTR, WT and

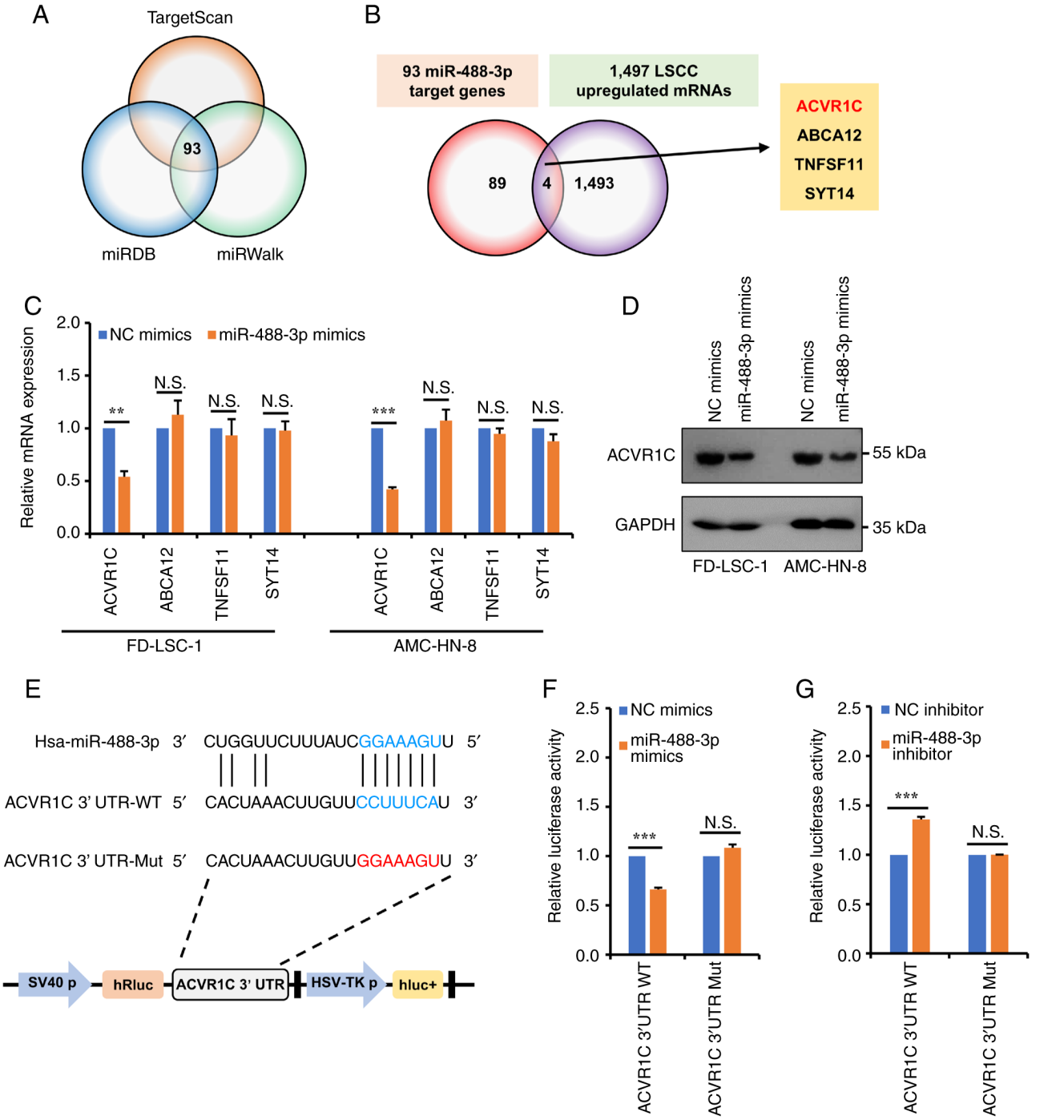

Figure 3. ACVR1C is a direct target gene of miR-488-3p. (A) Venn analysis of the target genes of miR-488-3p predicted by TargetScan, miRDB and miRWalk. (B) Venn analysis of the potential target genes of miR-488-3p and upregulated mRNAs in LSCC. (C) Quantitative PCR analysis of the mRNA levels of ACVR1C, ABCA12, TNFSF11 and SYT14 in LSCC cells transfected with miR-488-3p or NC mimics. (D) Western blotting of the protein levels of ACVR1C. (E) Schematic of ACVR1C 3' UTR sequence containing WT and Mut miR-488-3p binding sites. Luciferase reporter assay measured the luciferase activity of ACVR1C 3' UTR when FD-LSC-1 cells were transfected with miR-488-3p (F) mimics or (G) inhibitor. **P<0.01 and ***P<0.001. ACVR1C, activin A receptor type 1C; miR, microRNA; LSCC, laryngeal squamous cell carcinoma; NC, negative control; UTR, untranslated region; WT, wild type; Mut, mutant; N.S., not significant.

miR-488-3p binding-site Mut ACVR1C 3' UTRs were cloned into psiCHECK-2 vector for the dual-luciferase reporter assay (Fig. 3E). As shown in Fig. 3F, the luciferase activity was significantly decreased in FD-LSC-1 cells co-transfected with miR-488-3p mimics and the reporter vector harboring the WT ACVR1C 3' UTR, but not that harboring the Mut ACVR1C 3' UTR. By contrast, the miR-488-3p inhibitor significantly increased luciferase activity when co-transfected into cells with the WT ACVR1C 3' UTR reporter vector (Fig. 3G). These results indicated that miR-488-3p directly binds to ACVR1C 3' UTR.

ACVR1C knockdown inhibits LSCC cell proliferation, migration and invasion. ACVR1C has been implicated in

cell proliferation, migration and invasion in multiple types of cancer (21-24), but its role in LSCC remains unclear. Previous RNA-seq data (GSE127165) (11) indicated that ACVR1C was expressed at significantly higher levels in LSCC samples when compared with ANM tissues (Fig. 4A). To elucidate the effects of ACVR1C on LSCC, two specific siRNAs and a NC siRNA were transfected into FD-LSC-1 and AMC-HN-8 cells. The efficiency of ACVR1C knockdown was verified using qPCR and western blot analysis (Fig. 4B and C). As shown in Fig. 4D and E, ACVR1C knockdown significantly inhibited LSCC cell proliferation and colony formation. ACVR1C-knockdown AMC-HN-8 and FD-LSC-1 cells also exhibited reduced migration and invasion (Fig. 4F and G). Furthermore, increased expression of E-cadherin was observed in ACVR1C-knockdown LSCC cells, whereas the expression levels of vimentin and N-cadherin were decreased (Fig. 4H). These results indicated that ACVR1C knockdown could inhibit LSCC cell proliferation, migration, invasion and EMT.

miR-488-3p suppresses LSCC progression by targeting ACVR1C. Rescue experiments were designed to study whether miR-488-3p suppresses the malignant phenotype of LSCC cells by modulating ACVR1C. An ACVR1C overexpression plasmid and miR-488-3p mimics were transfected into FD-LSC-1 and AMC-HN-8 cells, either alone or in combination (Fig. 5A and B). Colony formation and CCK-8 assays showed that ACVR1C overexpression attenuated the inhibitory effects of miR-488-3p mimics on LSCC cell colony formation and proliferation (Fig. 5C and D). Similarly, it was found that ACVR1C overexpression rescued the suppressive effect of miR-488-3p on LSCC cell migration and invasion (Fig. 5E and F). These data indicated that miR-488-3p suppresses LSCC progression by negatively regulating ACVR1C expression.

miR-488-3p expression is regulated by MEIS1. The reason behind miR-488-3p downregulation in LSCC remains unclear. Thus, the promoter sequence (-2,000/-1) of miR-488 was downloaded from the UCSC Genome Browser and analyzed to identify conserved transcription factor binding sites. Two MEIS1-binding sites were identified in the core region of the miR-488-3p promoter (Fig. 6A) using the LASAGNA-Search 2.0 web tool (17) and JASPAR[2024] (jaspar.elixir.no/) database. Subsequent ChIP experiments demonstrated that MEIS1 significantly binds to the region of the miR-488 promoter that contains two MEIS1-binding sites, but not the NC region (Fig. 6B). Next, the sequences of the two MEIS1-binding sites were mutated and the targeting relationship was validated. Two luciferase reporter plasmids, named pGL3-488-WT and pGL3-488-Mut, were generated by inserting WT and MIES1-binding-site Mut miR-488 promoter (-2,000 to -1) into the pGL3-Basic vector. Luciferase reporter assays showed that overexpressing MEIS1 significantly increased the relative luciferase activity of the pGL3-488-WT vector in 293T cells, with no effect on the pGL3-488-Mut vector (Fig. 6C).

Furthermore, RNA-seq data (GSE127165) analysis showed that MEIS1 expression was significantly lower in LSCC tissues than in ANM tissues (Fig. 6D). Pearson's correlation analysis indicated that miR-488-3p levels were significantly positively correlated with MEIS1 in LSCC and ANM tissues (Fig. 6E). In addition, overexpression of MEIS1 significantly increased the levels of miR-488-3p in LSCC cells (Fig. 6F). Overall, these findings suggested that MEIS1 may bind directly to the miR-488-3p promoter and upregulate its expression in LSCC.

Downregulation of miR-488-3p partially reverses MEIS1-mediated tumor suppression. Previous studies have shown that MEIS1 has a tumor-suppressing effect in some cancers (25-27), but its role in LSCC remains unknown. To explore the effects of MEIS1 on LSCC, MEIS1 levels were upregulated by transfecting LSCC cells with MEIS1 overexpression plasmids. Meanwhile, to investigate whether MEIS1 exerts its function by regulating miR-488-3p expression, MEIS1 overexpression plasmids and a miR-488-3p inhibitor were simultaneously transfected into LSCC cells. WB confirmed that MEIS1 was overexpressed in AMC-HN-8 and FD-LSC-1 cells (Fig. 7A). qPCR indicated a significant reduction in miR-488-3p levels in the miR-488-3p inhibitor group compared with those in the NC group (Fig. 7B). As shown in Fig. 7C and D, MEIS1 overexpression suppressed the proliferative and colony-forming capacity of AMC-HN-8 and FD-LSC-1 cells, and that effect was partially recovered by the miR-488-3p inhibitor. In addition, Transwell assays demonstrated that overexpression of MEIS1 could suppress LSCC cell invasion and migration, whereas this was reversed in LSCC cells simultaneously transfected with MEIS1 overexpression plasmids and the miR-488-3p inhibitor (Fig. 7E and F). Collectively, these results revealed that MEIS1 could inhibit the malignant phenotype of LSCC cells, at least in part, by upregulating miR-488-3p expression.

miR-488-3p inhibits LSCC xenograft tumor growth in vivo. To further clarify whether miR-488-3p exerts its tumor-suppressive effect on LSCC *in vivo*, LSCC xenografts were established by subcutaneously injecting LSCC cells into the flanks of nude mice. A total of 10 days after inoculation, miR-488-3p or NC agomir was injected into the xenograft tumors every 2 days until day 22. As shown in Fig. 8A and B, LSCC xenograft tumors showed a significantly slower growth rate and lower weight in the miR-488-3p agomir-injected group compared with those in the NC agomir group. Subsequent RT-qPCR analysis indicated that miR-488-3p was expressed at higher levels in xenograft tumors injected with miR-488-3p agomir (Fig. 8C). Additionally, IHC staining showed that Ki67 expression in miR-488-3p agomir-injected tumor tissues was lower than that in the NC agomir group (Fig. 8D). Increased levels of E-cadherin in miR-488-3p agomir-injected tumor tissues were also observed, whereas the expression levels of N-cadherin and vimentin decreased, were indicating that upregulation of miR-488-3p inhibited EMT (Fig. 8D).

Discussion

Previous studies have demonstrated that miRNAs serve crucial regulatory roles in various diseases, especially cancer (5,28,29). Evidence has also accumulated for the clinical applications of miRNAs in cancer therapy. Our previous RNA-seq data showed that a large number of miRNAs are differentially expressed in LSCC tissues (11), indicating that miRNAs are

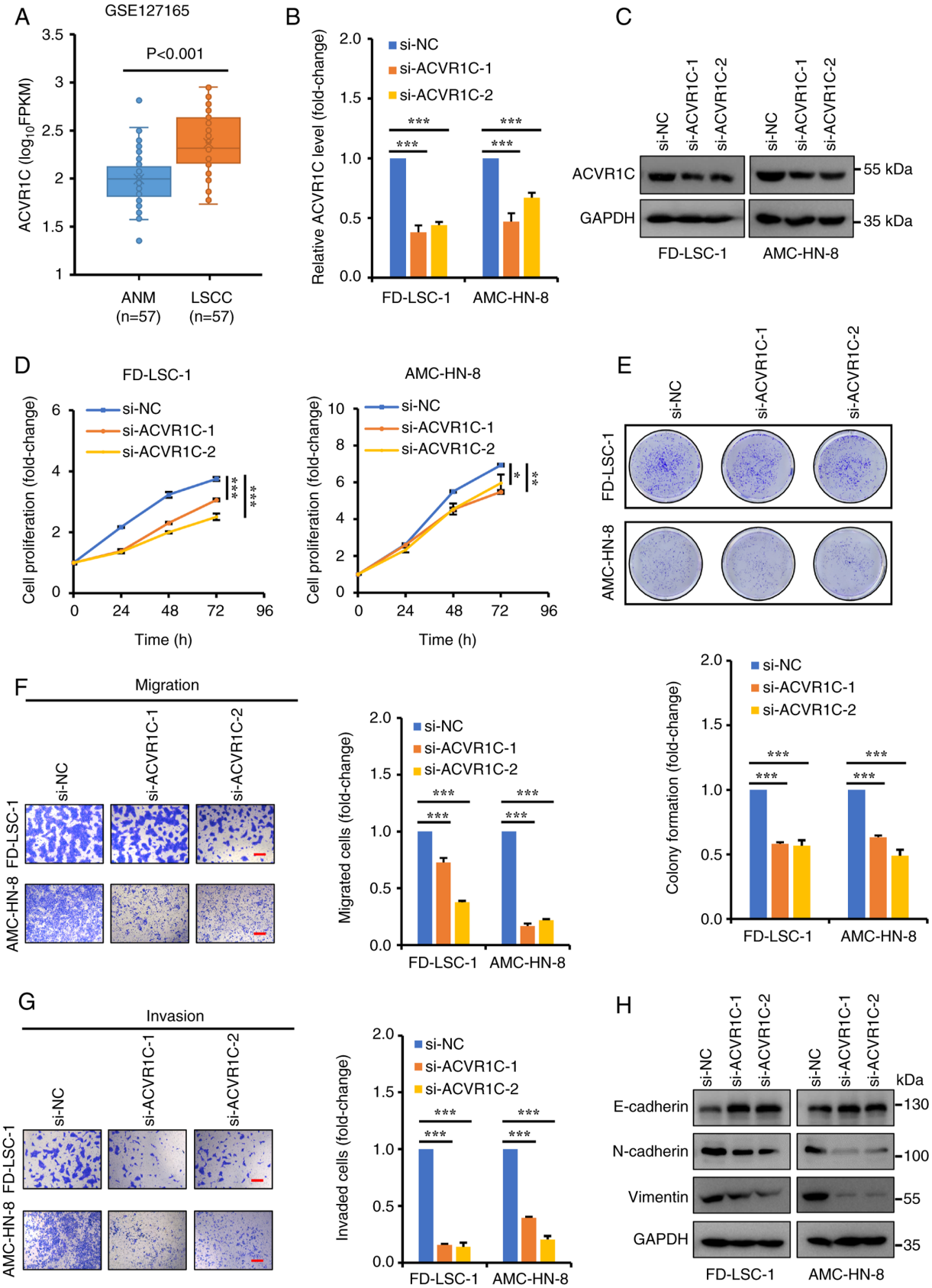

Figure 4. ACVR1C knockdown inhibits LSCC cell proliferation, migration, invasion and epithelial-mesenchymal transition. (A) Analysis of ACVR1C expression in RNA-seq data (GSE127165). (B) Quantitative PCR and (C) western blot analysis of the mRNA and protein expression levels of ACVR1C in AMC-HN-8 and FD-LSC-1 cells transfected with si-ACVR1C-1 and 2 or si-NC. Cropped images represent different blots, but samples are from the same experiment and the blots were processed in parallel. (D) Cell Counting Kit-8 and (E) colony formation assays investigated the proliferative ability of LSCC cells transfected with si-ACVR1C or si-NC. In the Transwell assay, ACVR1C knockdown significantly suppressed the (F) migration and (G) invasion of LSCC cells. (H) Western blot analysis of the protein levels of E-cadherin, N-cadherin and vimentin in LSCC cells transfected with si-ACVR1C or si-NC. Cropped images represent different blots, but samples are from the same experiment and the blots were processed in parallel. Scale bar, 100 μm. *P<0.05, **P<0.01 and ***P<0.001. ACVR1C, activin A receptor type 1C; LSCC, laryngeal squamous cell carcinoma; NC, negative control; si, small interfering RNA.

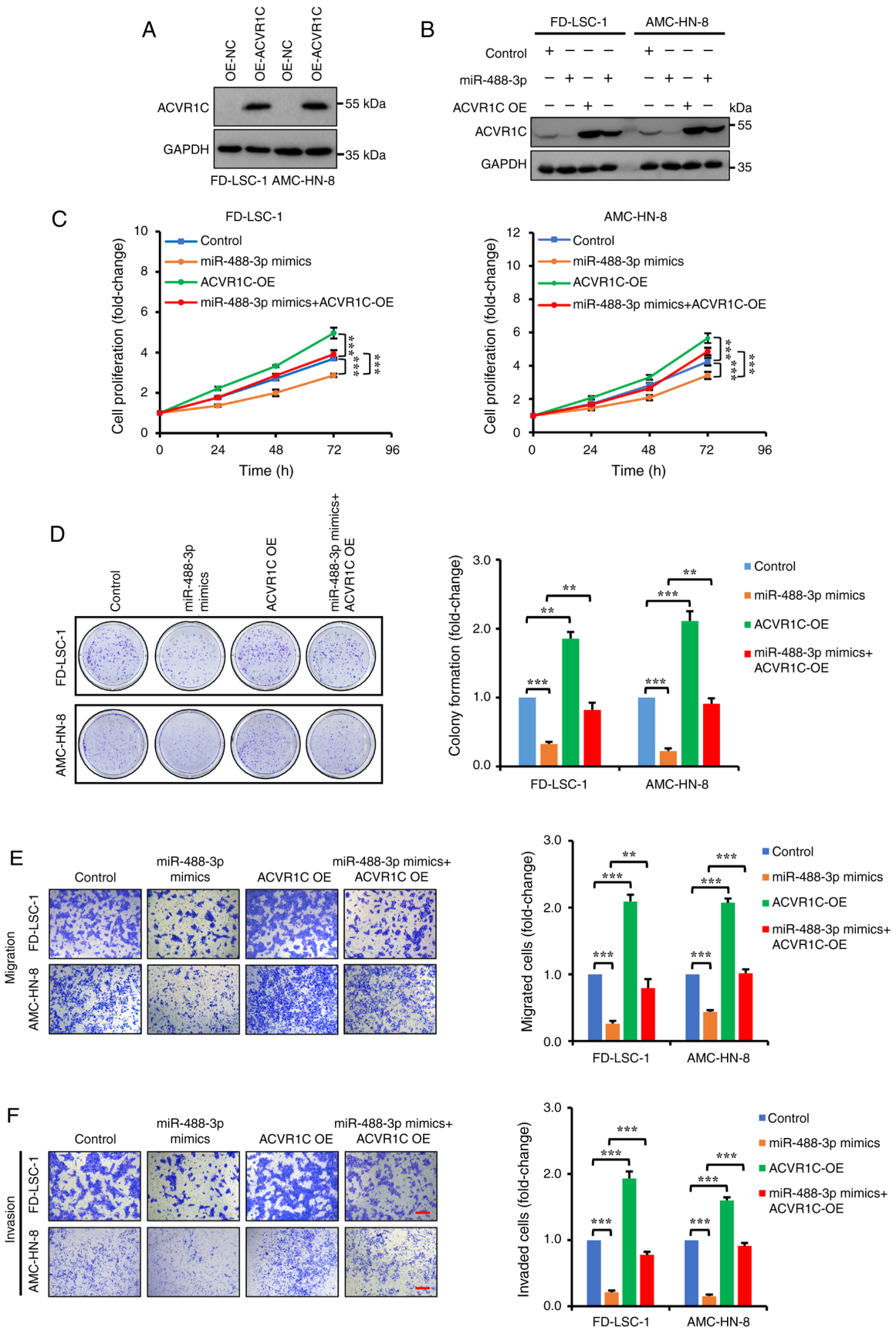

Figure 5. miR-488-3p suppresses LSCC cell proliferation, migration and invasion by targeting ACVR1C. (A) Western blot analysis of ACVR1C protein in FD-LSC-1 and AMC-HN-8 cells transfected with OE-ACVR1C or control empty plasmid (OE-NC). Flag antibodies were used to detect the Flag-tagged ACVR1C proteins. (B) Western blot analysis of ACVR1C protein expression in FD-LSC-1 and AMC-HN-8 cells co-transfected with OE-NC and NC mimics (Control), OE-NC and miR-488-3p mimics (miR-488-3p mimics), NC mimics and ACVR1C OE (ACVR1C OE) or miR-488-3p mimics and ACVR1C OE (miR-488-3p mimics + ACVR1C OE). (C) Cell Counting Kit-8 and (D) colony formation assays detected the proliferative ability of LSCC cells in different groups. (E and F) Transwell assays determined the migration and invasion of LSCC cells in different groups. Scale bar, 100 μm. **P<0.01 and ***P<0.001. ACVR1C, activin A receptor type 1C; miR, microRNA; LSCC, laryngeal squamous cell carcinoma; OE, overexpression.

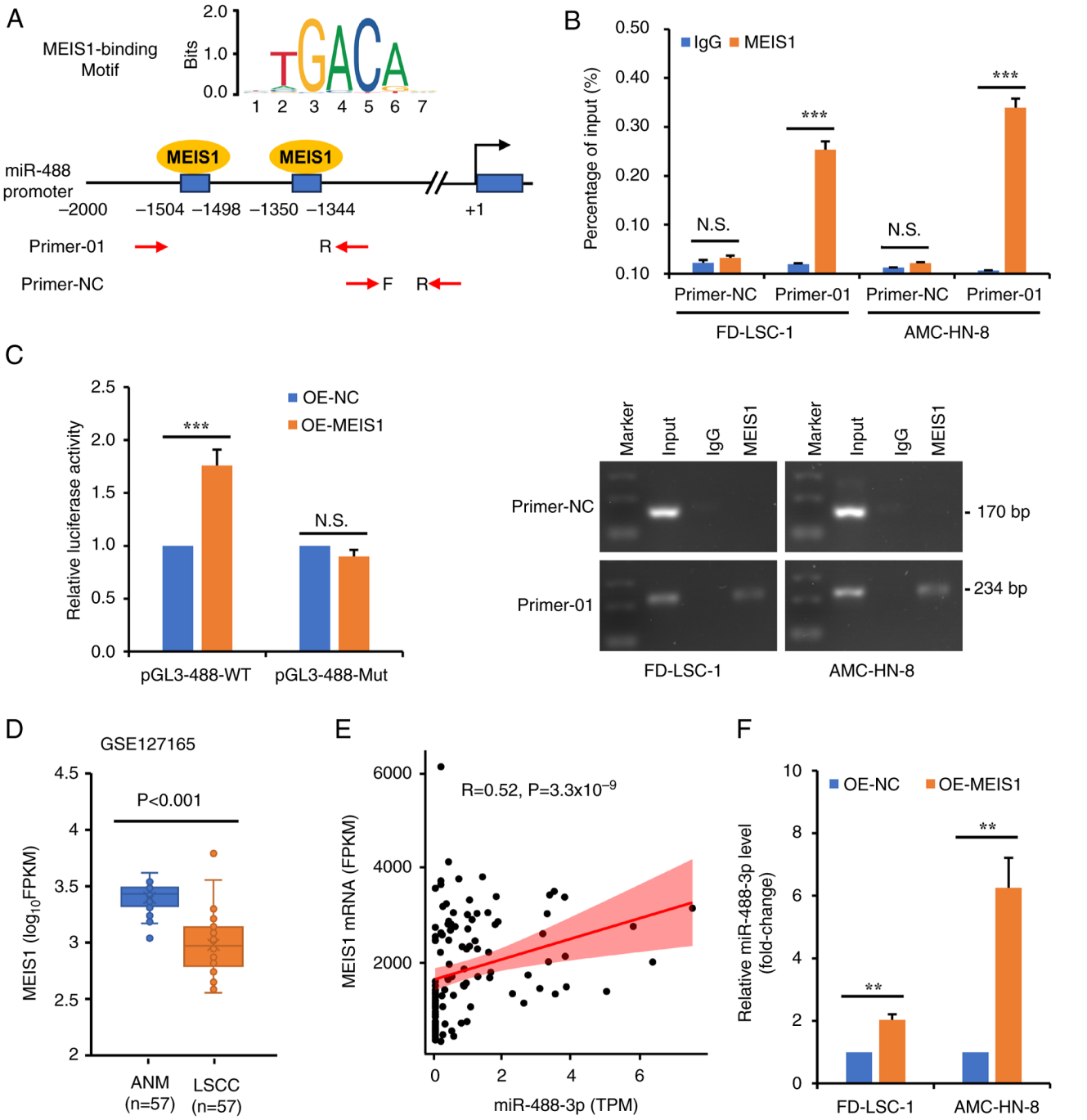

Figure 6. MEIS1 directly binds to the promoter region of miR-488 and upregulates the expression level of miR-488-3p. (A) Schematic of the core region of the miR-488 promoter and its potential MEIS1-binding sites. The binding sites for MEIS1 in the miR-488 promoter region were identified using the LASAGNA-Search 2.0 web tool and the JASPAR[2024] database. The MEIS1-binding motif was also taken from the JASPAR[2024] database. Primers were used to detect levels of miR-488 promoter fragments directly bound to MEIS1 in the ChIP assay. (B) ChIP-qPCR assay evaluated MEIS1-binding site interactions in the miR-488 promoter region. (C) Targeted relationship of MEIS1 to the miR-488 promoter was validated in 293T cells using dual-luciferase reporter gene assay. (D) Analysis of MEIS1 expression in RNA-seq data (GSE127165). (E) Correlation analysis of MEIS1 and miR-488-3p expression using RNA-seq data (GSE127165, GSE133632). (F) qPCR analysis of miR-488-3p expression in LSCC cells transfected with OE-MEIS1 or OE-NC. **P<0.01 and ***P<0.001. MEIS1, myeloid ecotropic viral integration site 1; N.S., not significant; miR, microRNA; qPCR, quantitative PCR; OE, overexpression; NC, negative control; LSCC, laryngeal squamous cell carcinoma; ChIP, chromatin immunoprecipitation.

involved in LSCC occurrence and development. Notably, the regulatory effects of numerous miRNAs in the carcinogenesis of LSCC have been investigated. For example, Gao *et al* (4,30) confirmed that miR-145-5p inhibits LSCC progression and chemoresistance by targeting different protein-coding genes. Wu *et al* (11,31) showed that overexpression of let-7c-5p and miR-1207-5p can inhibit the malignant phenotype of LSCC cells. In the present study, it was shown that miR-488-3p was downregulated in LSCC cell lines and tissues, and that its expression was associated with clinicopathological findings in patients with LSCC. Functional experiments indicated that miR-488-3p suppressed LSCC cell proliferation, migration, invasion, EMT and xenograft tumor growth. Mechanistically, ACVR1C was identified as a target gene of miR-488-3p, and

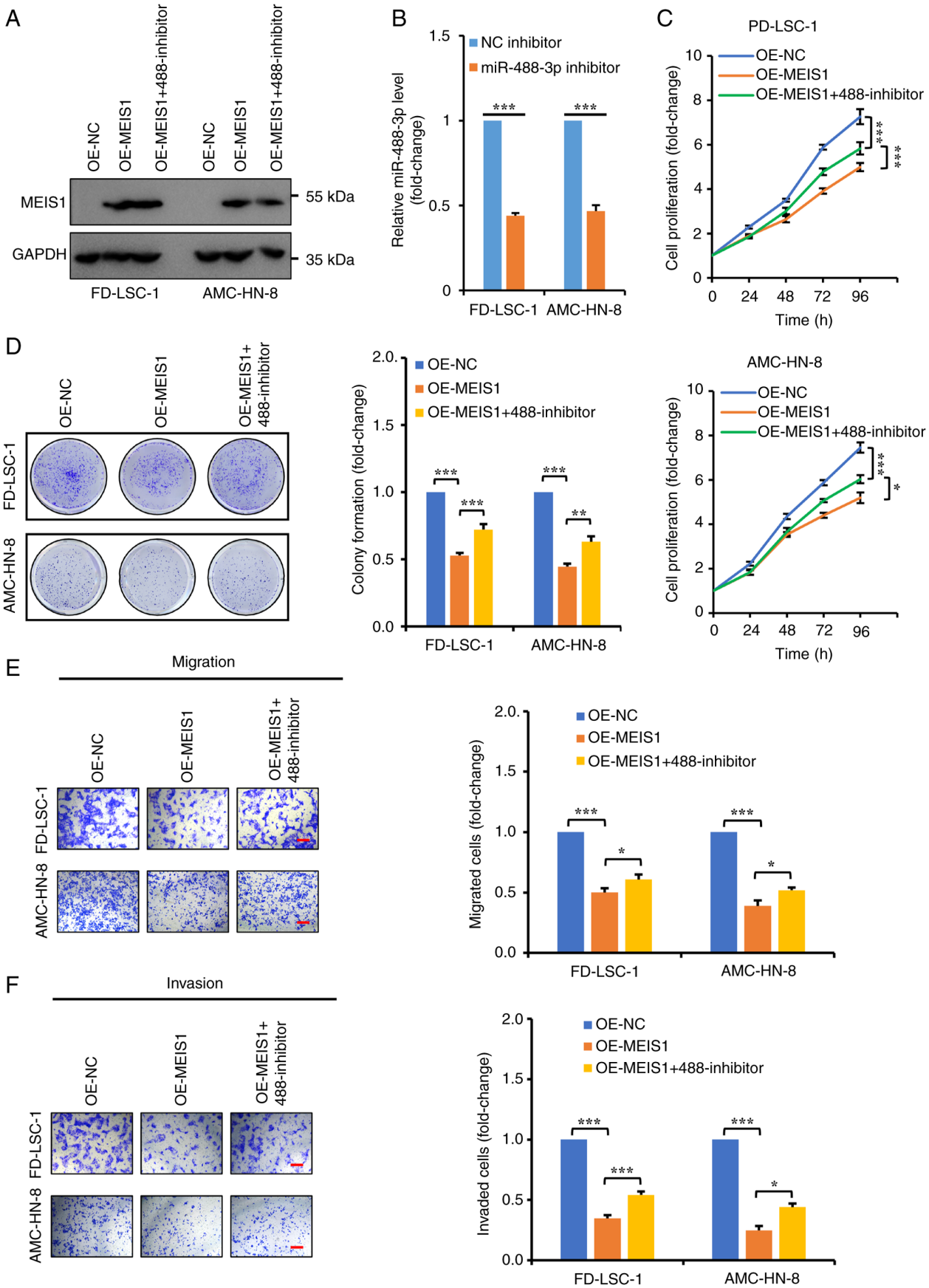

Figure 7. Downregulation of miR-488-3p partially reverses MEIS1-mediated tumor suppression. (A) Western blot analysis of MEIS1 protein in FD-LSC-1 and AMC-HN-8 cells transfected with OE-MEIS1 or co-transfected with OE-MEIS1 and miR-488-3p inhibitor. Flag antibodies were used to detect the Flag-tagged MEIS1 proteins. (B) qPCR analysis of miR-488-3p expression in LSCC cells transfected with miR-488-3p or NC inhibitors. (C) Cell Counting Kit-8 and (D) colony formation assays estimated the proliferative ability of LSCC cells in different groups. (E and F) Transwell assays determined the migration and invasion of LSCC cells in different groups. Scale bar, 100 μm. *P<0.05, **P<0.01 and ***P<0.001. MEIS1, myeloid ecotropic viral integration site 1; miR, microRNA; OE, overexpression; NC, negative control; LSCC, laryngeal squamous cell carcinoma.

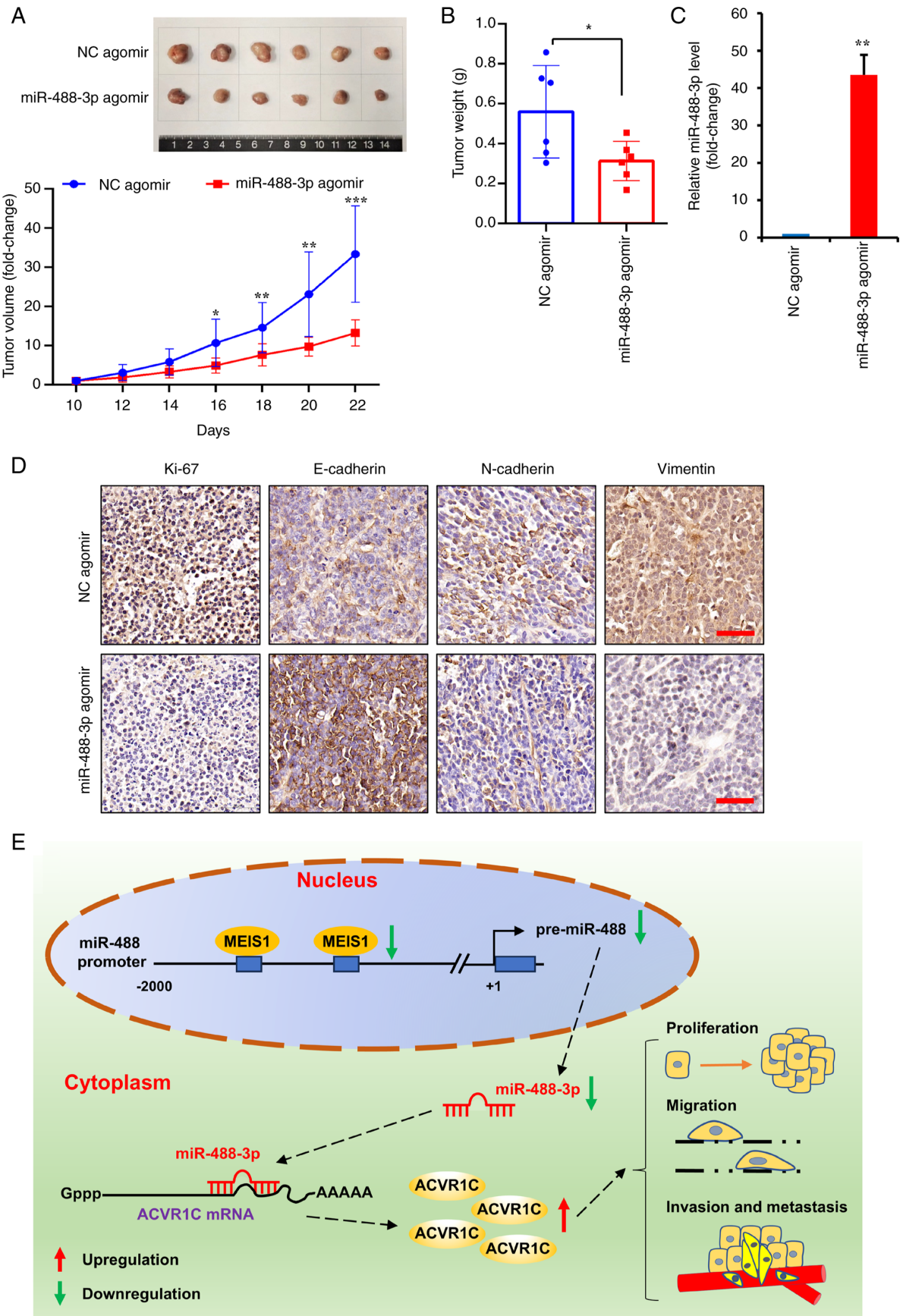

Figure 8. Effect of miR-488-3p on tumor growth *in vivo*. (A) Image of xenograft tumors after intratumoral injection of miR-488-3p or NC agomir. The xenograft tumor volume was measured to plot the growth curve. (B) Final weight of xenograft tumors. (C) Quantitative PCR analysis of miR-488-3p expression in xenograft tumors. (D) Representative immunohistochemical staining of vimentin, N-cadherin, E-cadherin and Ki-67 expression in xenograft tumors. (E) Schematic representation of the MEIS1/miR-488-3p/ACVR1C axis in regulating laryngeal squamous cell carcinoma progression. The red and green arrows indicate upregulation and downregulation in LSCC, respectively. Scale bar, 50 mm. *P<0.05, **P<0.01 and ***P<0.001. miR, microRNA; NC, negative control; MEIS1, myeloid ecotropic viral integration site 1; ACVR1C, activin A receptor type 1C.

ACVR1C could promote cell proliferation, migration, invasion and affect EMT. Furthermore, it was shown that MEIS1 upregulated miR-488-3p expression by directly binding to its promoter region. Rescue experiments demonstrated that downregulation of miR-488-3p partially reversed MEIS1-mediated tumor suppression.

The role of miR-488-3p in the pathogenesis and progression of cancer has been investigated for years, and its abnormal expression has been implicated in cancer progression, metastasis and survival (7). Previous studies have reported that miR-488-3p has tumor-suppressing effects in most human cancers (7,9,10,32). However, the exact function of miR-488-3p remains inconsistent in certain cancer types, with conflicting results shown in different studies of the same cancer (8,32-36). For example, in gastric cancer, multiple studies have revealed that miR-488-3p suppresses cell proliferation, migration and invasion (8,32,33), whereas another study came to the opposite conclusion (34). Similarly, Zhou *et al* (35) reported that miR-488-3p overexpression can promote cell proliferation while reducing apoptosis in osteosarcoma. However, another study reported that miR-488-3p suppresses osteosarcoma cell migration and invasion (36). These discrepancies may be attributed to variations in the sources of tissue samples and the cell lines used in these studies. Regarding LSCC, the expression, biological function and underlying mechanism of miR-488-3p in LSCC are still unclear. To the best of our knowledge, the present study is the first to report the tumor-suppressive effect of miR-488-3p on LSCC progression and EMT.

Our previous review article reported that miR-488-3p regulates various tumor cell phenotypes by targeting different genes (7). In the present study, ACVR1C was identified as a novel target of miR-488-3p in LSCC. ACVR1C, also known as activin-like kinase receptor 7, is a type I transforming growth factor-β (TGF-β) receptor, which can activate downstream SMAD signaling pathways by interacting with ligands and type II TGF-β receptors (22,37). The functional role of ACVR1C in cancer occurrence and development has also been previously reported (22). Hu *et al* (21) demonstrated that ACVR1C inhibits adhesion and proliferation in breast cancer cells, although the precise mechanism remains to be elucidated. In ovarian cancer, ACVR1C has been shown to suppress cell proliferation and induce apoptosis through regulation of the SMAD2/3 pathway (23,38-40). Conversely, ACVR1C has been implicated in oncogenic roles in certain cancers, such as pancreatic ductal adenocarcinoma (41), prolactinoma (24) and retinoblastoma (42). Notably, Asnaghi *et al* (42) demonstrated that ACVR1C facilitates the invasion and growth of retinoblastoma by activating the SMAD2 signaling pathway. According to the present findings, ACVR1C expression was significantly higher in LSCC tissues, and functional studies indicated that ACVR1C knockdown could suppresses LSCC cell proliferation, invasion, migration and EMT. It was also confirmed that miR-488-3p inhibited LSCC progression by downregulating ACVR1C.

The transcriptional regulatory mechanism of miR-488 expression has been reported on in several studies. Wu *et al* (43) reported that notch receptor 3 promotes miR-488 transcription in breast cancer by binding to the miR-488 promoter. Another study showed that nuclear factor κB inhibits miR-488 expression in pancreatic cancer by binding to its promoter region (44). In addition, in osteosarcoma, Zhou *et al* (35) reported that another transcription factor, HIF1-α, serves a key role in hypoxia-induced miR-488 transcription. To explore the transcriptional regulatory mechanism of miR-488-3p expression in LSCC, its promoter region was analyzed in the current study to identify transcription factor binding sites. In addition to the aforementioned transcription factors, two MEIS1-binding sites were detected in the miR-488 promoter region. As a transcription factor, evidence exists that MEIS1 functions as an oncogene in leukemia (45) but acts as a tumor suppressor in some types of cancer, such as clear cell renal cell carcinoma (25), non-small-cell lung cancer (26), prostate cancer (46) and colorectal cancer (47). Regarding the effects of MEIS1 on LSCC, it was first demonstrated that MEIS1 could promote miR-488-3p transcription by binding to its promoter. Furthermore, it was confirmed that MEIS1 overexpression suppressed LSCC cell proliferation, invasion and migration partially by upregulating miR-488-3p expression.

Furthermore, *in vivo* experiments revealed that miR-488-3p suppressed xenograft tumor growth. IHC staining results displayed an increased level of E-cadherin, and decreased levels of N-cadherin and vimentin in tumors injected with miR-488-3p agomir compared with control tissue. Collectively, the results highlighted the clinical implications of increased miR-488-3p expression for LSCC therapy.

Notably, the present study had several limitations. First, RNA-seq was not conducted to identify the target genes regulated by miR-488-3p in LSCC cells, which constrains the ability to achieve a comprehensive understanding of the mechanisms through which miR-488-3p influences LSCC progression. Second, further exploration of the downstream signaling pathways regulated by ACVR1C is warranted. Third, the partial reversal of MEIS1-mediated tumor suppression upon downregulation of miR-488-3p implies the involvement of additional molecules or signaling pathways in the MEIS1-mediated regulation of LSCC. Consequently, further research is necessary to fully elucidate the molecular mechanisms underlying the MEIS1/miR-488-3p/ACVR1C pathway in LSCC.

In conclusion, the current study revealed that miR-488-3p was significantly downregulated in both LSCC cell lines and tissues, and provided the first demonstration that miR-488-3p may inhibit the malignant properties of LSCC cells. Mechanistically, it was discovered for the first time, to the best of our knowledge, that miR-488-3p mediated by MEIS1 could exert its tumor-suppressive activity in LSCC by downregulating ACVR1C expression (Fig. 8E). These findings broaden the understanding of the functions and underlying mechanisms of miR-488-3p in LSCC progression and provide novel potential biomarkers or targets for the treatment of patients with LSCC.

Acknowledgements

Not applicable.

Funding

The present study was supported by the National Natural Science Foundation of China (grant no. 81802793), the Basic

Research Program of Shanxi Province (Free Exploration; grant nos. 202203021211015, 20210302124594, 202203021212045, 202203021212032 and 202203021212036), the Science Research Start-up Fund for Doctor of Shanxi Medical University (grant no. XD1801) and the National Clinical Research Center for Otorhinolaryngologic Diseases, Beijing, China (grant no. 2024KF003).

Availability of data and materials

The data generated in the present study may be requested from the corresponding author.

Authors' contributions

HL, LW and CZ designed the study and wrote the first draft of the manuscript. WH, XW, HG and LH performed most of the *in vitro* experiments. XZ and ZL conducted the bioinformatics analysis. WH, XW and YW performed the *in vivo* studies. HG, CZ and ZL contributed to clinical sample collection and data analysis. HL, QH and JY contributed to data analysis and tabulation. HL and CZ confirm the authenticity of all the raw data. All authors have read and approved the final version of the manuscript.

Ethics approval and consent to participate

The clinical samples were obtained with the written informed consent of patients and the study was approved by the Ethics Committee of the First Hospital of Shanxi Medical University (approval no. 2021-K-K005). Animal experiments were conducted according to the Health Guide for the Care and Use of Laboratory Animals approved by the Ethics Committee for Research Involving Animals of the First Hospital of Shanxi Medical University (approval no. DWYJ-2024-026).

Patient consent for publication

Not applicable.

Competing interests

The authors declare that they have no competing interests.

References

1. Johnson DE, Burtness B, Leemans CR, Lui VWY, Bauman JE and Grandis JR: Head and neck squamous cell carcinoma. Nat Rev Dis Primers 6: 92, 2020.
2. Steuer CE, El-Deiry M, Parks JR, Higgins KA and Saba NF: An update on larynx cancer. CA Cancer J Clin 67: 31-50, 2017.
3. Obid R, Redlich M and Tomeh C: The treatment of laryngeal cancer. Oral Maxillofac Surg Clin North Am 31: 1-11, 2019.
4. Gao W, Zhang C, Li W, Li H, Sang J, Zhao Q, Bo Y, Luo H, Zheng X and Lu Y, *et al*: Promoter methylation-regulated miR-145-5p inhibits laryngeal squamous cell carcinoma progression by targeting FSCN1. Mol Ther 27: 365-379, 2019.
5. Di Leva G, Garofalo M and Croce CM: MicroRNAs in cancer. Annu Rev Pathol 9: 287-314, 2014.
6. Lu TX and Rothenberg ME. MicroRNA. J Allergy Clin Immunol 141: 1202-1207, 2018.
7. Yang J, Wang X, Hao W, Wang Y, Li Z, Han Q, Zhang C and Liu H: MicroRNA-488: A miRNA with diverse roles and clinical applications in cancer and other human diseases. Biomed Pharmacother 165: 115115, 2023.
8. Luo M, Deng X, Chen Z and Hu Y: Circular RNA circPOFUT1 enhances malignant phenotypes and autophagy-associated chemoresistance via sequestrating miR-488-3p to activate the PLAG1-ATG12 axis in gastric cancer. Cell Death Dis 14: 10, 2023.
9. Fang C, Chen YX, Wu NY, Yin JY, Li XP, Huang HS, Zhang W, Zhou HH and Liu ZQ: MiR-488 inhibits proliferation and cisplatin sensibility in non-small-cell lung cancer (NSCLC) cells by activating the eIF3a-mediated NER signaling pathway. Sci Rep 7: 40384, 2017.
10. Deng X, Li D, Ke X, Wang Q, Yan S, Xue Y, Wang Q and Zheng H: Mir-488 alleviates chemoresistance and glycolysis of colorectal cancer by targeting PFKFB3. J Clin Lab Anal 35: e23578, 2021.
11. Wu Y, Zhang Y, Zheng X, Dai F, Lu Y, Dai L, Niu M, Guo H, Li W, Xue X, *et al*: Circular RNA circCORO1C promotes laryngeal squamous cell carcinoma progression by modulating the let-7c-5p/PBX3 axis. Mol Cancer 19: 99, 2020.
12. Wu CP, Zhou L, Gong HL, Du HD, Tian J, Sun S and Li JY: Establishment and characterization of a novel HPV-negative laryngeal squamous cell carcinoma cell line, FD-LSC-1, with missense and nonsense mutations of TP53 in the DNA-binding domain. Cancer Lett 342: 92-103, 2014.
13. Livak KJ and Schmittgen TD: Analysis of relative gene expression data using real-time quantitative PCR and the 2(-Delta Delta C(T)) Method. Methods 25: 402-408, 2001.
14. McGeary SE, Lin KS, Shi CY, Pham TM, Bisaria N, Kelley GM and Bartel DP: The biochemical basis of microRNA targeting efficacy. Science 366: eaav1741, 2019.
15. Chen Y and Wang X: miRDB: An online database for prediction of functional microRNA targets. Nucleic Acids Res 48: D127-D131, 2020.
16. Sticht C, De La Torre C, Parveen A and Gretz N: miRWalk: An online resource for prediction of microRNA binding sites. PLoS One 13: e0206239, 2018.
17. Lee C and Huang CH: LASAGNA-Search: An integrated web tool for transcription factor binding site search and visualization. Biotechniques 54: 141-153, 2013.
18. Rauluseviciute I, Riudavets-Puig R, Blanc-Mathieu R, Castro-Mondragon JA, Ferenc K, Kumar V, Lemma RB, Lucas J, Chèneby J, Baranasic D, *et al*: JASPAR 2024: 20th anniversary of the open-access database of transcription factor binding profiles. Nucleic Acids Res 52(D1): D174-D182, 2024.
19. Perez G, Barber GP, Benet-Pages A, Casper J, Clawson H, Diekhans M, Fischer C, Gonzalez JN, Hinrichs AS, Lee CM, *et al*: The UCSC Genome Browser database: 2025 update. Nucleic Acids Res 53: D1243-D1249, 2025.
20. Amin MB, Greene FL, Edge SB, Compton CC, Gershenwald JE, Brookland RK, Meyer L, Gress DM, Byrd DR and Winchester DP: The Eighth Edition AJCC cancer staging manual: Continuing to build a bridge from a population-based to a more 'personalized' approach to cancer staging. CA Cancer J Clin 67: 93-99, 2017.
21. Hu T, Su F, Jiang W and Dart DA: Overexpression of activin receptor-like kinase 7 in breast cancer cells is associated with decreased cell growth and adhesion. Anticancer Res 37: 3441-3451, 2017.
22. Du R, Wen L, Niu M, Zhao L, Guan X, Yang J, Zhang C and Liu H: Activin receptors in human cancer: Functions, mechanisms, and potential clinical applications. Biochem Pharmacol 222: 116061, 2024.
23. Xu G, Zhou H, Wang Q, Auersperg N and Peng C: Activin receptor-like kinase 7 induces apoptosis through up-regulation of Bax and down-regulation of Xiap in normal and malignant ovarian epithelial cell lines. Mol Cancer Res 4: 235-246, 2006.
24. Principe M, Chanal M, Karam V, Wierinckx A, Mikaélian I, Gadet R, Auger C, Raverot V, Jouanneau E, Vasiljevic A, *et al*: ALK7 expression in prolactinoma is associated with reduced prolactin and increased proliferation. Endocr Relat Cancer 25: 795-806, 2018.
25. Zhu J, Cui L, Xu A, Yin X, Li F and Gao J: MEIS1 inhibits clear cell renal cell carcinoma cells proliferation and in vitro invasion or migration. BMC Cancer 17: 176, 2017.
26. Li W, Huang K, Guo H and Cui G: Meis1 regulates proliferation of non-small-cell lung cancer cells. J Thorac Dis 6: 850-855, 2014.
27. VanOpstall C, Perike S, Brechka H, Gillard M, Lamperis S, Zhu B, Brown R, Bhanvadia R and Vander Griend DJ: MEIS-mediated suppression of human prostate cancer growth and metastasis through HOXB13-dependent regulation of proteoglycans. Elife 9: e53600, 2020.

28. Peng Y and Croce CM: The role of MicroRNAs in human cancer. Signal Transduct Target Ther 1: 15004, 2016.
29. Kulkarni B, Kirave P, Gondaliya P, Jash K, Jain A, Tekade RK and Kalia K: Exosomal miRNA in chemoresistance, immune evasion, metastasis and progression of cancer. Drug Discov Today 24: 2058-2067, 2019.
30. Gao W, Guo H, Niu M, Zheng X, Zhang Y, Xue X, Bo Y, Guan X, Li Z, Guo Y, *et al*: circPARD3 drives malignant progression and chemoresistance of laryngeal squamous cell carcinoma by inhibiting autophagy through the PRKCI-Akt-mTOR pathway. Mol Cancer 19: 166, 2020.
31. Wu Y, Dai F, Zhang Y, Zheng X, Li L, Zhang Y, Cao J and Gao W: miR-1207-5p suppresses laryngeal squamous cell carcinoma progression by downregulating SKA3 and inhibiting epithelial-mesenchymal transition. Mol Ther Oncolytics 22: 152-165, 2021.
32. Zhao Y, Lu G, Ke X, Lu X, Wang X, Li H, Ren M and He S: miR-488 acts as a tumor suppressor gene in gastric cancer. Tumour Biol 37: 8691-8698, 2016.
33. Yang D, Shi M, You Q, Zhang Y, Hu Z, Xu J, Cai Q and Zhu Z: Tumor- and metastasis-promoting roles of miR-488 inhibition via HULC enhancement and EZH2-mediated p53 repression in gastric cancer. Cell Biol Toxicol 39: 1341-1358, 2023.
34. Wang D, Su F and Feng M: Circular RNA hsa_circ_0000751 serves as a microRNA-488 sponge to suppress gastric cancer progression via ubiquinol-cytochrome c reductase core protein 2 regulation. Bioengineered 12: 8793-8808, 2021.
35. Zhou C, Tan W, Lv H, Gao F and Sun J: Hypoxia-inducible microRNA-488 regulates apoptosis by targeting Bim in osteosarcoma. Cell Oncol (Dordr) 39: 463-471, 2016.
36. Bu J, Guo R, Xu XZ, Luo Y and Liu JF: LncRNA SNHG16 promotes epithelial-mesenchymal transition by upregulating ITGA6 through miR-488 inhibition in osteosarcoma. J Bone Oncol 27: 100348, 2021.
37. Schmierer B and Hill CS: TGFbeta-SMAD signal transduction: Molecular specificity and functional flexibility. Nat Rev Mol Cell Biol 8: 970-982, 2007.
38. Ye G, Fu G, Cui S, Zhao S, Bernaudo S, Bai Y, Ding Y, Zhang Y, Yang BB and Peng C: MicroRNA 376c enhances ovarian cancer cell survival by targeting activin receptor-like kinase 7: Implications for chemoresistance. J Cell Sci 124: 359-368, 2011.
39. Xu G, Bernaudo S, Fu G, Lee DY, Yang BB and Peng C: Cyclin G2 is degraded through the ubiquitin-proteasome pathway and mediates the antiproliferative effect of activin receptor-like kinase 7. Mol Biol Cell 19: 4968-4979, 2008.
40. Xu G, Zhong Y, Munir S, Yang BB, Tsang BK and Peng C: Nodal induces apoptosis and inhibits proliferation in human epithelial ovarian cancer cells via activin receptor-like kinase 7. J Clin Endocrinol Metab 89: 5523-5534, 2004.
41. Nguyen DT, Lee E, Alimperti S, Norgard RJ, Wong A, Lee JJ, Eyckmans J, Stanger BZ and Chen CS: A biomimetic pancreatic cancer on-chip reveals endothelial ablation via ALK7 signaling. Sci Adv 5: eaav6789, 2019.
42. Asnaghi L, White DT, Key N, Choi J, Mahale A, Alkatan H, Edward DP, Elkhamary SM, Al-Mesfer S, Maktabi A, *et al*: ACVR1C/SMAD2 signaling promotes invasion and growth in retinoblastoma. Oncogene 38: 2056-2075, 2019.
43. Wu Y, Yuan MH, Wu HT, Chen WJ, Zhang ML, Ye QQ, Liu J and Zhang GJ: MicroRNA-488 inhibits proliferation and motility of tumor cells via downregulating FSCN1, modulated by Notch3 in breast carcinomas. Cell Death Dis 11: 912, 2020.
44. Han D, Zhu S, Li X, Li Z, Huang H, Gao W, Liu Y, Zhu H and Yu X: The NF-κB/miR-488/ERBB2 axis modulates pancreatic cancer cell malignancy and tumor growth through cell cycle signaling. Cancer Biol Ther 23: 294-309, 2022.
45. Yokoyama T, Nakatake M, Kuwata T, Couzinet A, Goitsuka R, Tsutsumi S, Aburatani H, Valk PJ, Delwel R and Nakamura T: MEIS1-mediated transactivation of synaptotagmin-like 1 promotes CXCL12/CXCR4 signaling and leukemogenesis. J Clin Invest 126: 1664-1678, 2016.
46. Bhanvadia RR, VanOpstall C, Brechka H, Barashi NS, Gillard M, McAuley EM, Vasquez JM, Paner G, Chan WC, Andrade J, *et al*: MEIS1 and MEIS2 expression and prostate cancer progression: A role for HOXB13 binding partners in metastatic disease. Clin Cancer Res 24: 3668-3680, 2018.
47. Li Y, Gan Y, Liu J, Li J, Zhou Z, Tian R, Sun R, Liu J, Xiao Q, Li Y, *et al*: Downregulation of MEIS1 mediated by ELFN1-AS1/EZH2/DNMT3a axis promotes tumorigenesis and oxaliplatin resistance in colorectal cancer. Signal Transduct Target Ther 7: 87, 2022.